

Controlled Placement of Individual Carbon Nanotubes

Xue Ming Henry Huang,[†] Robert Caldwell,[‡] Limin Huang,[‡] Seong Chan Jun,[†]
Mingyuan Huang,[†] Matthew Y. Sfeir,[§] Stephen P. O'Brien,[‡] and James Hone^{*†}

Departments of Mechanical Engineering, Applied Physics, and Chemistry; Nanoscale Science & Engineering Center and Materials Research Science & Engineering Center, Columbia University, New York, New York 10027

Received May 12, 2005; Revised Manuscript Received June 9, 2005

ABSTRACT

A central challenge for both the science and the technology of carbon nanotubes is the controlled assembly of devices. Here, we report a technique that allows us to place a nanotube with the desired properties in a predetermined location by direct mechanical transfer. We demonstrate single-tube and multiple-tube transfer and electrical characterization of an optically characterized nanotube. The ability to rationally design nanotube devices and circuits will enable more detailed study of the physics and chemistry of nanotubes and provide a stepping stone toward implementation of a wide spectrum of applications.

Because of their outstanding electrical, thermal, and mechanical properties, single-walled carbon nanotubes (SWCNTs) hold promise for a number of applications and are of great interest as a model nanoscale system.^{1,2} However, the controlled “bottom-up” assembly of nanotube devices and structures remains a significant challenge: It is difficult to control the exact placement of nanotubes on a surface, and chiral angle (which determines semiconducting or metallic character) cannot be chosen a priori. Early SWNT devices were fabricated by depositing bulk-grown SWNTs from liquid suspension,³ either on top of prepatterned electrodes or directly onto a substrate prior to electrode patterning. This process has the advantages of low cost, scalability, and compatibility with many substrate materials. However, it has significant disadvantages, including randomness in both nanotube placement and chiral species. Furthermore, it generally requires ultrasonic agitation that breaks the SWNTs into small pieces ($\sim 1 \mu\text{m}$ or shorter). Large efforts are underway worldwide to address many of these challenges (for instance, by chemical modification of the substrate for nanotube self-assembly⁴), but the goal of fully controlled placement of nanotubes with specific chiral index and arbitrary length remains elusive. Alternatively, SWNTs can be grown directly on a substrate by chemical vapor deposition (CVD).⁵ CVD can produce SWNTs with lengths up to a few centimeters,⁶ with reasonable control over location, orientation, and diameter. Notably, with control of growth direction,

nanotube networks can be built by sequential growth at different orientations of the same chip. However, it is still difficult to control chirality and the subsequent electronic properties. Furthermore, many substrates, including glass, flexible plastics, and standard silicon complementary metal oxide semiconductor (CMOS) chips, will not withstand the temperatures (700–900 °C) required for high-quality SWNT synthesis.

Here, we describe a mechanical transfer technique that circumvents many of the limitations of both suspension-casting and direct CVD growth^{7–9} by separating the two processes. In addition, the technique achieves precise control over both the type and the location of the nanotube. Briefly, long nanotubes are grown by CVD across a narrow slit etched through a Si wafer. The suspended sections are characterized optically to determine their electronic structure. A specific nanotube can then be chosen and placed on another substrate with micron-scale precision by putting the two substrates in contact at the desired location.

The first step in the sample fabrication process consists of the growth of freely suspended nanotubes, as shown in Figure 1. The growth substrate consists of a Si wafer with Si_3N_4 epilayers on both sides. Standard bulk micromachining is used to etch from the back of the wafer and define a long, thin membrane on the top. The membrane is removed by ultrasonication to create a slit in the chip. A catalyst consisting of bimetallic CoMo-doped mesoporous silica (SBA-16) is placed on one side of the chip by stamping. Ethanol CVD growth generates long, aligned SWNTs¹⁰ that traverse the slit. Scanning electron microscopy (SEM) micrographs of a nanotube crossing a slit are shown in Figure 1. Figure 1a shows the entire width of a slit; at this

* To whom correspondence should be addressed. E-mail: jh2228@columbia.edu.

[†] Mechanical Engineering.

[‡] Applied Physics.

[§] Chemistry.

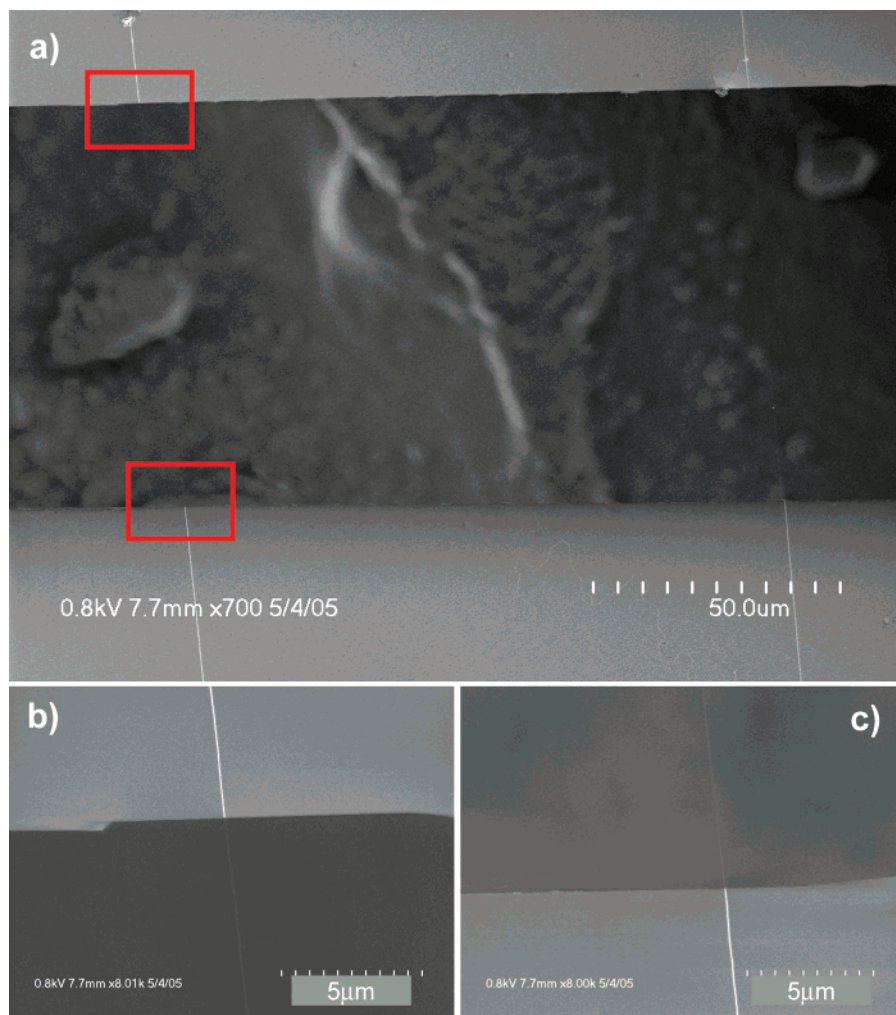


Figure 1. Ethanol-based CVD growth of long SWNTs. (a) SEM image taken at low magnification, showing long nanotubes grown across a slit, whose length is essentially limited by the size of the chip (the structure inside the slit is the conductive carbon tape used to affix the sample in the SEM). (b, c) Zoom-in views of a local region near the edges of the slit, showing nanotubes traversing the gap.

magnification, the nanotube is only visible on top of the solid substrate. At higher magnification (Figure 1b,c), the nanotube can clearly be seen to traverse the slit. The suspended nanotubes are remarkably robust: We have observed SWNTs suspended across slits up to 0.5 mm wide.

Following growth, the electronic properties and structure of the suspended nanotubes can be determined. The diameter of the SWNTs was estimated to be in the range 0.8–2.4 nm from the radial breathing mode (RBM) peaks of Raman scattering spectra at 632.8 and 514 nm excitations. In fact, the suspended tube geometry permits characterization by multiple techniques, including Rayleigh scattering,¹¹ Raman scattering,^{11,12} and spectrofluorimetry,¹³ as well as imaging techniques such as high-resolution transmission electron microscopy and electron diffraction.¹⁴ Here, we focus on the use of Rayleigh scattering. At present, this technique allows for the rapid identification of semiconducting and metallic tubes and can discriminate between individual SWNTs and bundles; soon, it should be possible to perform complete (n, m) structural assignment by this technique. On each chip, a Rayleigh spectrum is first collected for each SWNT crossing the slit. Next, a specific nanotube with the desired properties

is selected. The remaining nanotubes are then burned away by positioning the illumination spot (diameter $\sim 5 \mu\text{m}$) over each one at high intensity. Because the suspended tubes are generally separated by tens of microns, it is easy to avoid burning the chosen tube, so that it can then be transferred in the next step.

The process for nanotube mechanical transfer is depicted in Figure 2. The ends of the suspended SWNT section are coated with 30 nm gold, using a shadow mask (Figure 2a). The gold coating renders the nanotube ends visible in an optical microscope (inset). Next, the growth chip is inverted, positioned using a mask aligner, and finally put into contact with the target chip at the desired location (Figure 2b). To hold the nanotube in place on the target chip, a small amount of photoresist is applied to the target area through the back of the slit and cured in situ. Apart from photoresist, we have also demonstrated the applicability of alternative resist materials, such as the poly(methyl methacrylate) (PMMA), a commonly used electron beam resist. The use of standard resist material in this process demonstrates its compatibility with microchip industrial production. The two chips are then separated, leaving the suspended nanotube section affixed

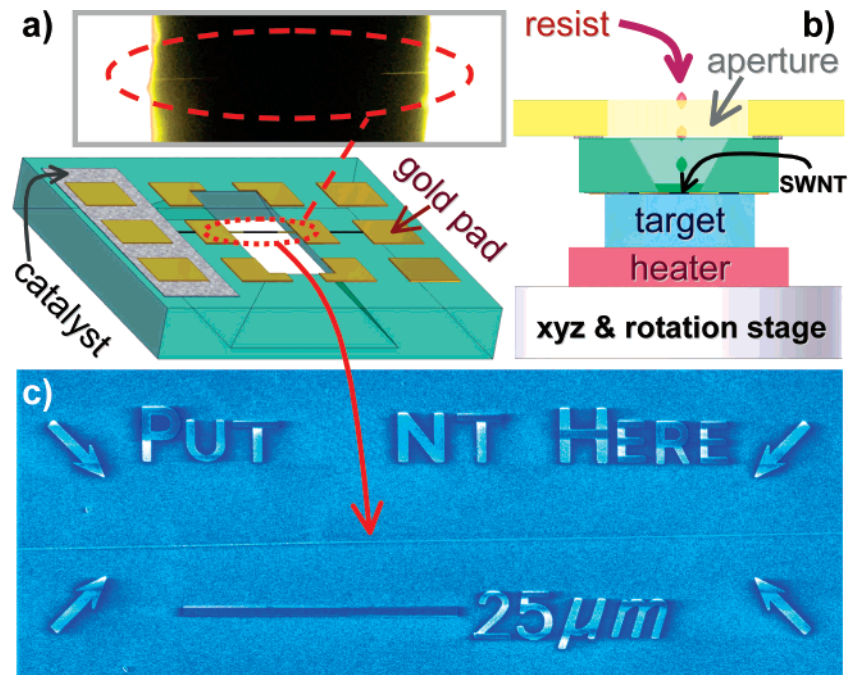


Figure 2. Mechanical transfer of a long SWNT from the CVD growth chip to a target chip. (a) Growth chip schematics. (inset) Optical image showing a suspended nanotube $160\ \mu\text{m}$ long. The gold-coated ends are clearly visible. (b) Schematic drawing of the transfer process. (c) SEM image of a target chip after nanotube transfer and resist removal, showing micron scale accuracy.

to the target substrate by the resist. Finally, the resist is gently removed, leaving the nanotube in the desired location on the surface of the target chip.

Figure 2c shows an SEM image of a single nanotube transferred onto a target chip with predefined metal alignment markers (text, scale bar, and arrows). The transferred nanotube is about $160\ \mu\text{m}$ long (the image shows only the center section) and is placed at the center of the pattern with $\sim 2\ \mu\text{m}$ accuracy. When photoresist is used to hold down the transferred tube, the transfer technique is highly reliable, and we have reproduced these results a number of times with very few processing errors. Alternatively, the nanotube can be transferred without photoresist, in which case the process relies upon van der Waals adhesion of the suspended section to the target chip. This “dry” process is also effective but is somewhat less reliable because of the smaller forces that hold the nanotube down. Ongoing work is being undertaken to determine the maximum placement accuracy achievable by this technique, which will depend on both optical resolution and mechanical factors such as vibration. Because the center of an object can be located with significantly better accuracy than the diffraction limit, it is certainly plausible that this technique could achieve placement accuracy in the range of tens of nanometers.

We have also demonstrated the ability to manipulate a particular nanotube with preselected properties. Figure 3a shows the Rayleigh spectrum for a single nanotube before transfer, indicating semiconducting bandstructure. The tube was then transferred to a quartz substrate and patterned with source and drain leads by electron beam lithography and liftoff processes. A 50 nm layer of aluminum oxide was deposited on top of the chip by atomic layer deposition (ALD). Finally, a second e-beam lithography and liftoff

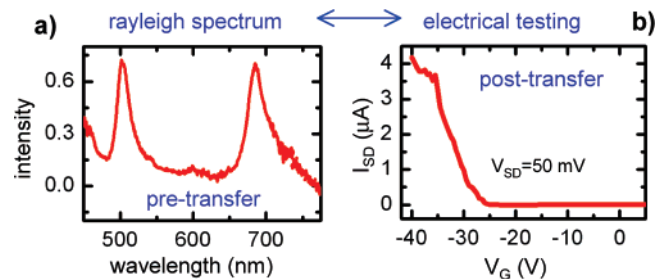


Figure 3. Optical vs electrical. (a) Rayleigh spectrum of a single nanotube before transfer, indicating semiconducting band structure. (b) Semiconducting transport characteristics of the same nanotube after transfer.

process was used to define a top gate. Figure 3b shows the low-bias current through the device as a function of voltage to the top gate. The transport data indicate semiconducting behavior, as predicted by optical spectroscopy.

Because of the high accuracy and repeatability of the process, we have also been able to build multiple-nanotube structures by repeated transfer. Figure 4 shows the simple network structures we have built by sequentially transferring a few nanotubes onto a target substrate at different orientations. Because it is possible to construct devices out of preselected nanotubes, it will be possible to build many types of complex multi-nanotube devices,¹⁵ for instance, prototype all-nanotube integrated circuits, which are not feasible with random deposition. The use of long nanotubes, in combination with demonstrated placement precision, makes it possible to build large networks of chosen nanotubes by sequential controlled placement.

This initial demonstration clearly shows the level of control we have achieved over these tiny entities, in terms of both

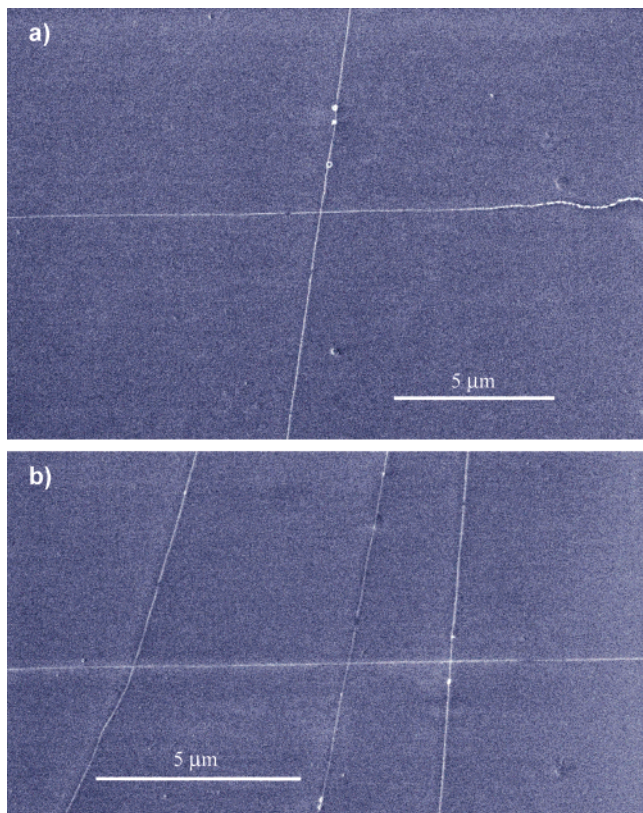


Figure 4. Simple network of nanotubes made by the transfer technique. (a) A cross-junction of two nanotubes. (b) Several nanotubes crossing one, potentially applicable as noninvasive electrical contacts for transport studies.

nanotube species and physical location. Even at this early stage, the technique described above constitutes an important research tool for the study of SWNTs, in that it permits the construction of single- and multiple-tube devices using well-characterized individual nanotubes. In addition, the transfer process circumvents the temperature restrictions associated with CVD, permitting device fabrication on glass and plastic and allowing for direct integration of long SWNTs with prefabricated CMOS chips. Therefore, this method offers a

unique route toward guided assembly of next-generation hybrid nanosystems, especially at the prototyping level.

Acknowledgment. This work was supported primarily by the Nanoscale Science and Engineering Initiative of the National Science Foundation under NSF award no. CHE-0117752 and by the New York State Office of Science, Technology, and Academic Research (NYSTAR). The work has used shared experimental facilities supported primarily by the MRSEC program of the National Science Foundation under award no. DMR-0213574. We thank Prof. L. Brus and Prof. T. Heinz for use of equipment for Rayleigh scattering spectroscopy.

References

- (1) Saito, R.; Dresselhaus, G.; Dresselhaus, M. S. *Physical Properties of Carbon Nanotubes*; Imperial College Press: Singapore, 2001.
- (2) Iijima, S. *Nature (London)* **1991**, *354*, 56–58.
- (3) Tans, S. J.; Verschueren, A. R. M.; Dekker, C. *Nature (London)* **1998**, *393*, 49–52.
- (4) Auvray, S.; Derycke, V.; Goffman, M.; Filoramo, A.; Jost, O.; Bourgoin, J.-P. *Nano Lett.* **2005**, *5*, 451–455.
- (5) Dai, H. J. *Top. Appl. Phys.* **2001**, *80*, 29–53.
- (6) Zheng, L. X.; O'Connell, M. J.; Doorn, S. K.; Liao, X. Z.; Zhao, Y. H.; Akhadow, E. A.; Hoffbauer, M. A.; Roop, B. J.; Jia, Q. X.; Dye, R. C.; Peterson, D. E.; Huang, S. M.; Liu, J.; Zhu, Y. T. *Nat. Mater.* **2004**, *3*, 673–676.
- (7) Hines, D. R.; Mezheny, S.; Brebran, M.; Williams, E. D.; Ballarotto, V. W.; Esen, G.; Southard, A.; Fuhrer, M. S. *Appl. Phys. Lett.* **2005**, *86*, 163101.
- (8) Bradley, K.; Gabriel, J. C. P.; Gruner, G. *Nano Lett.* **2003**, *3*, 1353–1355.
- (9) Meitl, M. A.; Zhou, Y. X.; Gaur, A.; Jeon, S.; Usrey, M. L.; Strano, M. S.; Rogers, J. A. *Nano Lett.* **2004**, *4*, 1643–1647.
- (10) Huang, L. M.; Cui, X.; White, B.; O'Brien, S. P. *J. Phys. Chem. B* **2004**, *108*, 16451.
- (11) Sfeir, M. Y.; Wang, F.; Huang, L. M.; Chuang, C. C.; Hone, J.; O'Brien, S. P.; Heinz, T. F.; Brus, L. E. *Science* **2004**, *306*, 1540–1543.
- (12) Dresselhaus, M. S.; Dresselhaus, G.; Saito, R.; Jorio, A. *Phys. Rep.* **2005**, *409*, 47–99.
- (13) Bachilo, S. M.; Strano, M. S.; Kittrell, C.; Hauge, R. H.; Smalley, R. E.; Weisman, R. B. *Science* **2002**, *298*, 2361–2366.
- (14) Zuo, J. M.; Vartanyants, I.; Gao, M.; Zhang, R.; Nagahara, L. A. *Science* **2003**, *300*, 1419–1421.
- (15) Fuhrer, M. S.; Nygard, J.; Shih, L.; Forero, M.; Yoon, Y. G.; Mazzoni, M. S. C.; Choi, H. J.; Ihm, J.; Louie, S. G.; Zettl, A.; McEuen, P. L. *Science* **2000**, *288*, 494–497.

NL050886A